Materials and Design 197 (2021) 109203

Contents lists available at ScienceDirect

Materials and Design

journal homepage: www.elsevier.com/locate/matdes

Simple fabrication of highly sensitive capacitive pressure sensors using a porous dielectric layer with cone-shaped patterns

Yeongjun Kim, Hyeondong Yang, Je Hoon Oh *

Department of Mechanical Engineering, Hanyang University, 55 Hanyangdaehak-ro, Sangnok-gu, Ansan, Gyeonggi-do 15588, Republic of Korea

HIGHLIGHTS

- Fabrication of porous structures in a PDMS film with cone-shaped surface patterns using simple microwave irradiation.
- Combination effect of highly deformable characteristics and varying dielectric constant for high sensitivity of the sensors.
- Finite element analysis for optimization of the distance between cone-shaped patterns.
- Excellent performance for future applications such as sensor array and skin attached sensors for wearable electronics.

GRAPHICAL ABSTRACT

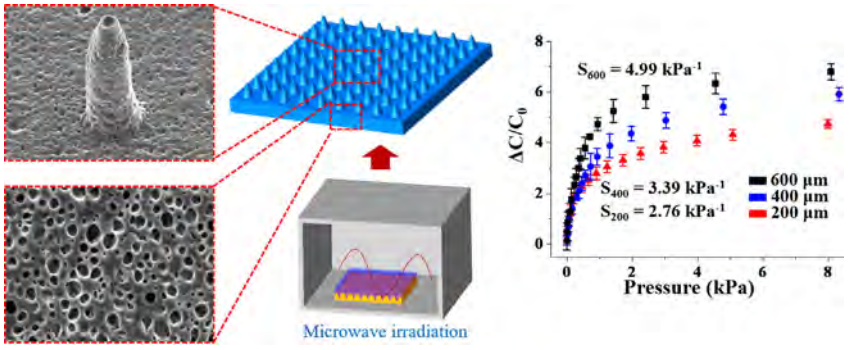

ARTICLE INFO

Article history:
Received 24 August 2020
Received in revised form 29 September 2020
Accepted 30 September 2020
Available online 2 October 2020

Keywords:
Polydimethylsiloxane
Porous structures
Capacitive pressure sensors
Wearable electronics

ABSTRACT

This study aims to improve the sensitivity of sensors using porous structures and cone-shaped patterns in the composition of a capacitive pressure sensor. A simple and rapid fabrication method for the production of porous structures and cone-shaped patterns using microwave irradiation of emulsions containing polydimethylsiloxane (PDMS) and a sacrificial solvent is introduced in this study. Through this method, a porous PDMS dielectric layer could be simply fabricated within a few minutes. The sensitivity was greatly improved by both enhancing deformability and increasing the dielectric constant under the external pressure. The effect of pattern distance was investigated, and the sensor with the pattern distance of 600 μm showed a remarkably high sensitivity of approximately 5 kPa^{-1}. Moreover, the effect of aspect ratio and sharpness of the patterns were also studied through a finite element analysis. Finally, we demonstrated the performance of the sensor using a sensor array and finger attached sensors, and they showed sufficient performance for use in wearable devices applicable to artificial skin, surgical robots, and pressure monitoring systems, among others.

1. Introduction

Numerous research, in recent years, has investigated wearable electronics and artificial skin that is capable of measuring temperature [1,2], humidity [3,4], strain [5,6], and pressure [7,8]. In order to measure these external stimuli, a sensor corresponding to each stimulus is required, and many researchers are trying to improve the performance of the sensors for more realistic and practical applications. In particular, pressure sensors have been actively studied due to a large amount of data available from the sensors and their applicability to various fields [9,10]. Pressure sensors can be categorized as piezoelectric [11–15], resistive [16–21], or capacitive [7,8,22–26]. Among them, capacitive pressure sensors have been attracting the most attention because of their simple structure, low power consumption, and excellent stability.

* Corresponding author.
E-mail address: jehoon@hanyang.ac.kr (J.H. Oh).

https://doi.org/10.1016/j.matdes.2020.109203

The biggest challenge of the capacitive pressure sensor is to achieve high sensitivity to be applicable to artificial skin and wearable electronics. Since the capacitive pressure sensor has the sandwiched structure of electrode-dielectric-electrode and works by measuring the capacitance variation which is inversely proportional to the distance between two electrodes, sufficient deformability of the dielectric layer is highly demanded for high sensitivity. Polydimethylsiloxane (PDMS) is the most widely used dielectric materials for capacitive pressure sensors because it is highly deformable, eco-friendly, transparent, and biocompatible, which makes it especially suitable as artificial skin. Despite the excellent deformability of the PDMS, sensors using bulk PDMS showed insufficient sensitivity for use in wearable electronics. Many studies have aimed to improve the deformability of the PDMS dielectric layer to produce highly sensitive capacitive pressure sensors.

Some researchers enhanced the deformability of the dielectric layer by patterning microstructures on the surface of the layer [8]. Molds fabricated through the photolithography processes were usually used for this method. They achieved relatively high sensitivity, but the complicated and expensive processes were required to manufacture molds. Baek et al. modified the surface of the PDMS layer via ultraviolet (UV) treatment [27]. The UV irradiation was performed on the surface of the pre-strained PDMS film. A thin silicon oxide layer could be obtained through the UV irradiation, and the wavy patterns were fabricated after removing the strain due to the buckling of the surface. This method was a simple and easy way to modify the surface structures, however, the sensitivity of the sensors was still insufficient.

Lin et al. fabricated PDMS core-shell nanofiber using the electrospinning technique, and the nanofiber was used as a dielectric layer of a capacitive pressure sensor [28]. The sensor showed a sensitivity of 0.43 kPa^{-1}. Our group fabricated a pressure sensor with electrospun poly(vinylidenefluoride-*co*-trifluoroethylene) (PVDF-TrFE) nanofibers, and the sensitivity of 2.81 kPa^{-1} was obtained [22]. Electrospinning is a promising technique to fabricate porous structures, however, electrospun nanofibers have relatively low adhesion force, resulting in delamination between the nanofibers and a substrate. Besides, a few hours of spinning time are needed to obtain sufficient thickness of the nanofiber layer.

A particle template method is an alternative to form porous structures in a PDMS dielectric film for a capacitive pressure sensor. In this method, the porous structures were formed by curing PDMS with dissolvable particles, such as sugar, salt, and polystyrene beads, and then removing these particles using water or dimethylformamide [29–34]. This method is a relatively simple method compared to other methods to fabricate porous structures, however, it requires complex manufacturing processes and large amounts of time up to 24 h. In addition, the sensitivities of the sensors were not sufficiently high. Thus, a simple and efficient way to fabricate porous structures inside a PDMS dielectric layer is still necessary for highly sensitive pressure sensors.

In this study, we present a simple fabrication method to produce a porous structured PDMS dielectric layer with improved deformability, resulting in highly sensitive pressure sensors. The porous structures were prepared using microwave irradiation of an emulsion consisting of a sacrificial solvent and a pre-cured PDMS solution. With this method, uniformly distributed porous structures can be easily formed in a few minutes. The absence of a post-process in the microwave irradiation method allows for an extremely shortened fabrication time. in addition, by transferring con-shaped patterns on the surface of the dielectric layer, the sensitivity of the sensor can be further improved. A sensor array and finger-attached sensors were also fabricated and evaluated; they showed excellent performance as artificial skin.

2. Experimental section

2.1. Preparation of a dielectric layer

Fig. 1 shows the schematic illustration of the fabrication process of the PDMS dielectric layer. The porous structured PDMS dielectric layer with cone-shaped patterns was produced by microwave irradiation of the PDMS emulsion, which contained perfluorocarbon (FC-42, 3 M) as a sacrificial solvent. A glass mold was prepared by ultraviolet (UV) treatment of photo-sensitive glass with dimensions of 30 by 30 mm (Foturan®, SCHOTT Co.). Once the glass was exposured to UV light, the lighted spot is melted. After the etching process using a 10% aqueous hydrofluoric (HF) acid solution at 25 °C, the conical patterns were engraved. The PDMS prepolymer and curing agent (Sylgard 184, Dow Chemical Co.) were firstly mixed at a ratio of 20:1, and FC-43 was dispersed in a pre-PDMS solution at a concentration of 0 vol% to 50 vol%

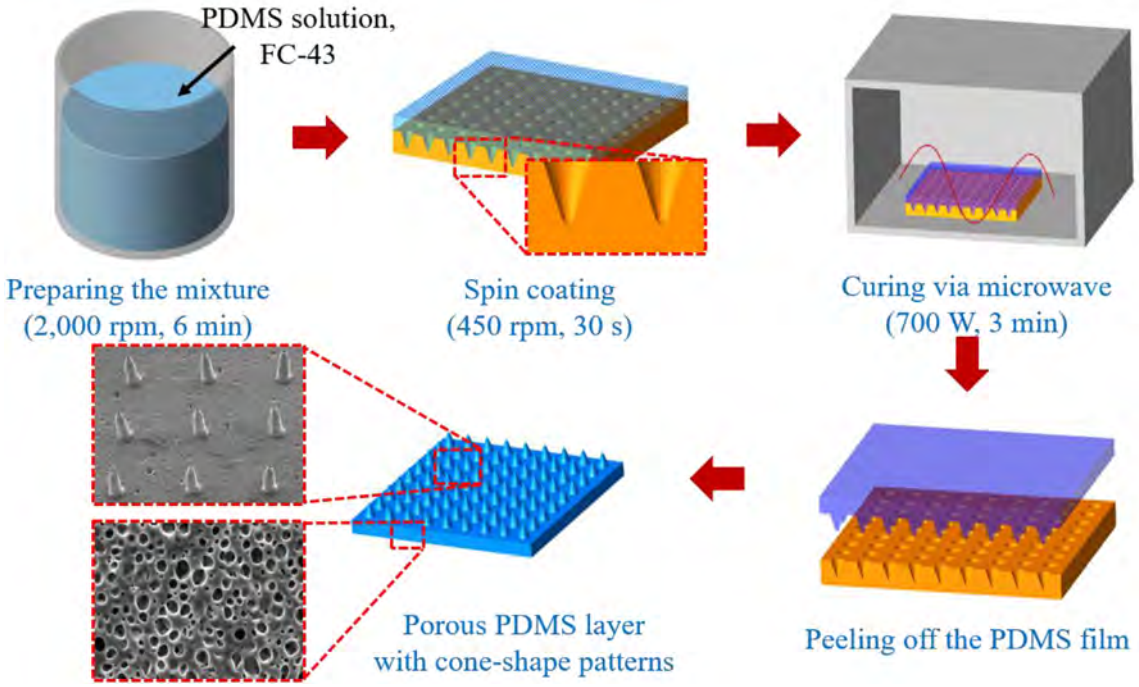

Fig. 1. Schematic of the fabrication process of a porous PDMS film with cone-shaped patterns.

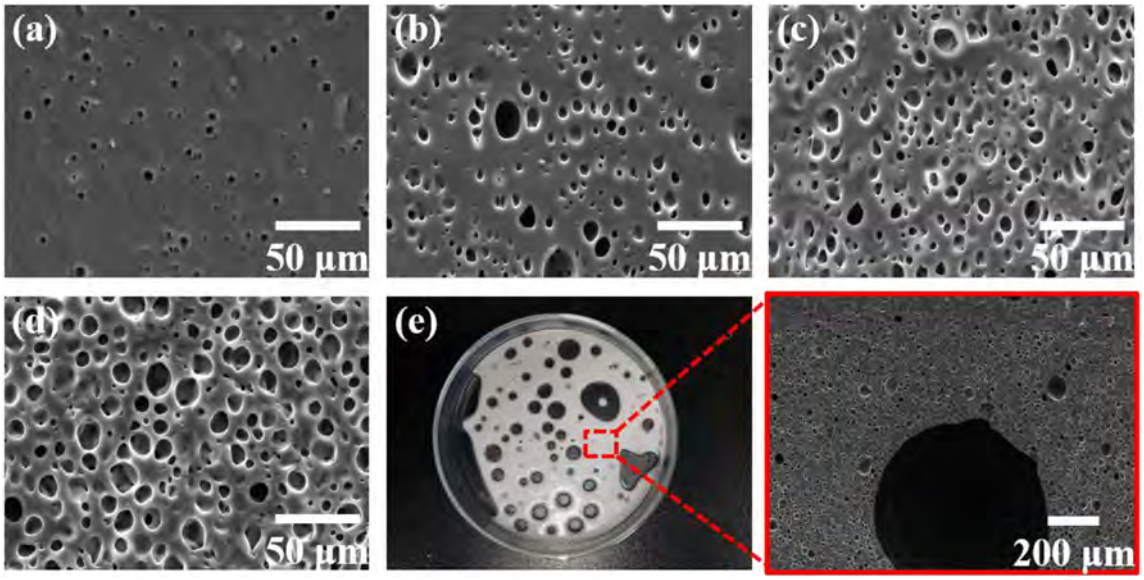

Fig. 2. Cross-sectional SEM images of the porous PDMS dielectric layer with FC-43 ratios of (a) 10 vol%, (b) 20 vol%, (c) 30 vol%, and (d) 40 vol%. (e) An ununiform film produced with an FC-43 ratio of 50 vol%. SEM image in the red box shows the cross-sectional view of the sample.

with an interval of 10 vol% to fabricate the PDMS emulsion. The emulsion was mechanically mixed for 6 min at 2000 rpm using a homo-mixer (ARE-310, Thinky Co.). The emulsion of 1 mL was poured on the glass mold and spin-coated at 450 rpm for 30 s. The sample was then degassed in a vacuum for 10 min to remove any residual air. The fabrication of the PDMS dielectric layer was completed after microwave irradiation for 3 min using a household microwave oven. The microwave irradiation was conducted in a fume hood to prevent hazardous gases from forming during the fabrication process. The fabricated porous PDMS film with cone-shaped patterns had a total thickness of 200 μm.

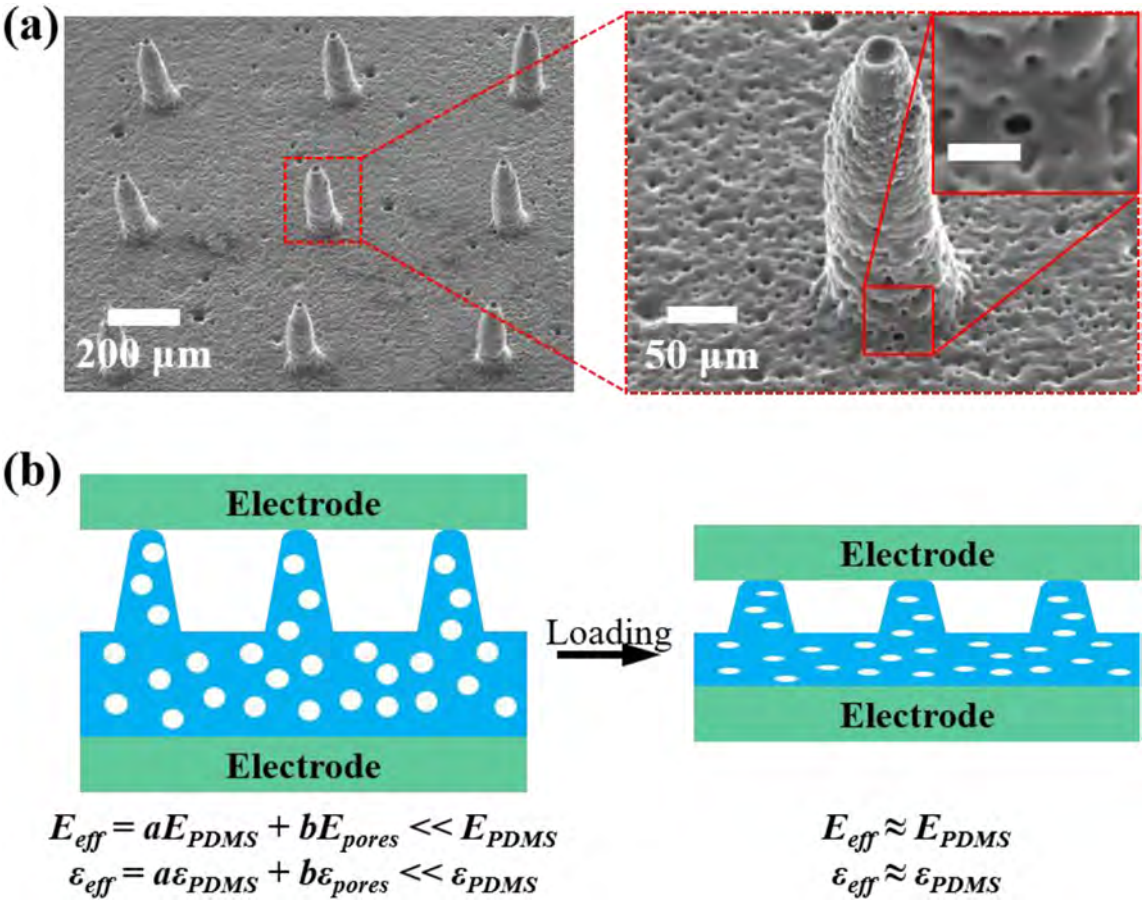

Fig. 3. (a) SEM images of transferred cone-shaped patterns with the distance of 400 μm. The scale bar in the inset image is 20 μm. (b) Schematic of the deformation of the dielectric layer under pressure, and the change of the effective Young's modulus and dielectric constant of the layer.

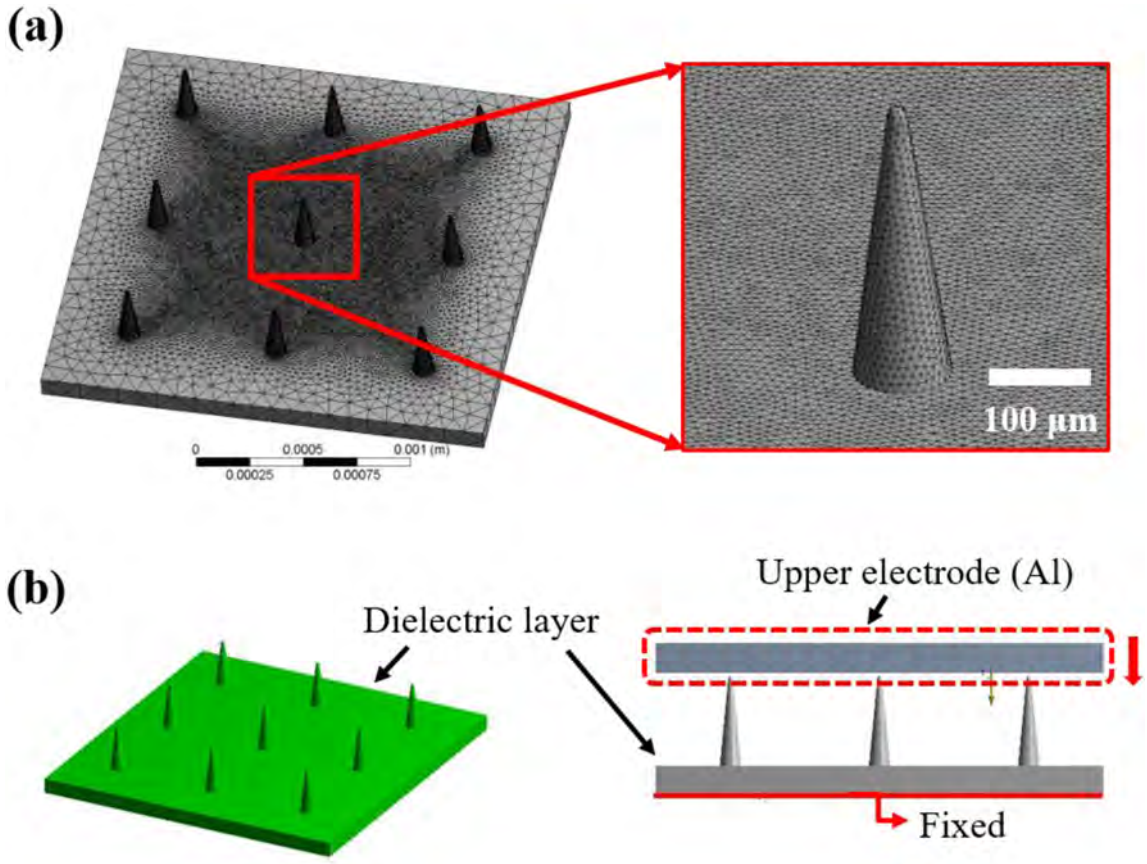

Fig. 4. (a) A tetrahedron mesh used for the FEA. (b) A model for the FEA and the boundary conditions.

2.2. Fabrication of a capacitive pressure sensor and sensor array

The capacitive pressure sensor was fabricated using the aforementioned PDMS dielectric layer. An aluminum (Al) fabric was used as an electrode to secure the flexibility of the sensor, and it was bonded with a PDMS substrate using a silicone epoxy. The PDMS dielectric layer was sandwiched between two electrodes, bonded using a PDMS solution, and cured at 70 °C for 4 h. the overlapping area of the two electrodes was 10 mm by 10 mm. the PDMS substrate with an Al electrode had a thickness of 400 μm, so the fabricated sensor had a total thickness of 1 mm. Copper wires were connected to the electrodes using silver epoxy.

The sensor array was fabricated in the same manner as above, in which Al electrodes having a width of 3 mm were bonded with the PDMS substrate. The distance between the Al electrodes was set to be 3 mm. Four electrodes on the top and four electrodes on the bottom were placed perpendicular to each other.

2.3. Characterization and evaluation

Capacitance values under external pressure were measured using an LCR meter (IM-3523, HIOKI), and the external load was applied using an in-house *Z*-axis stage. The applied force on a sensor was measured with the help of a load cell (UMM-K20, Dacell Co.) installed at the stage. The entire fabrication and measurement were implemented at a humidity of 25% and room temperature.

3. Results and discussion

3.1. Porous dielectric layer with cone-shaped patterns

The difference in pore formation inside the dielectric layer was firstly investigated as a function of the sacrificial solvent ratio using field emission-scanning electron microscope (FE-SEM, MIRA3, TESCAN). As shown in Fig. 2, micro-pores were well generated in the PDMS layer. The FC-43 molecule was strongly vibrated and rapidly heated by the microwave irradiation. FC-43 was then transformed from its liquid phase into gas phase. Micro-pores were formed since the phase change of the sacrificial solvent and curing process of PDMS simultaneously progress. The PDMS can be rapidly cured due to internally generated heat from microwave irradiation, which causes micropores to be trapped in the PDMS layer. It should be noted that other methods of fabricating a porous structure required time-consuming processes because they needed additional processes along with the curing of PDMS, but in the method proposed in this paper, curing of the PDMS and fabrication of the porous structure were carried out simultaneously within 3 min.

Pores were uniformly generated in the PDMS film, and the pore size and porosity increased with increasing the ratio of the FC-43 (Supplementary Material Fig. S1). It is more likely that the pores of adjacent solvent regions would coalesce as more solvent was added during the fabrication of the dielectric layer. The pore size and porosity were almost proportional to the solvent ratio, which means that they can be easily controlled. However, when the ratio of the FC-43 was higher than 50 vol%, the solvent and PDMS were not completely dispersed, resulting in the solvent macroscopically separating from the PDMS. A non-uniform porous structure was fabricated when this sample was microwave-irradiated as shown in Fig. 2(e).

The pores greatly improved the deformability of the layer; this was further enhanced with the cone-shaped patterns (Fig. 3(a)). The pores not only improved the deformability of the layer but also resulted in varying dielectric constants of the film under external pressure (Fig. 3(b)). As external pressure was applied to the sensor, the pores closed, thereby increasing the dielectric constant of the entire film as the amount of eliminated pores increased. Capacitive pressure sensors

operate by measuring capacitance values, which are proportional to the overlapping area of the electrodes (A) and the dielectric constant (ε) of the dielectric layer (in this work, the PDMS film) and are inversely proportional to the distance between the two electrodes (d). The improved deformability of the pores increased the variation of the value of d when pressure was applied; the change in the capacitance value further increased due to the increase in the dielectric constant by the elimination of pores. The distance between the cone-shape patterns, i.e. the frequency of the patterns, would affect the deformability of the dielectric layer. We conducted finite element analysis (FEA) to observe the effect of the distance of the patterns on the deformability and the microscopic behavior of the patterns under compressive deformation.

3.2. FEA simulation of the pattern's behavior under compressive deformation

A tensile test was firstly conducted to investigate the effect of the FC-43 ratio on Young's modulus of PDMS film. FC-43 was mixed with a PDMS solution from 0 vol% to 50 vol% with an interval of 10 vol%. For the test, dog-bone samples were prepared using the aforementioned fabrication procedure. A manual universal test machine (HTC-10000 N, Smart Control & Sensing Co.), a load cell (UU-K500, Dacell Co.), and a linear variable differential transformer (CDP-100, TML Co.) were used. As a result of the test, a decrease in Young's modulus could be observed with an increase of FC-43 ratio (Supplementary Material Fig. S2). The reduction in Young's modulus was due to the size and frequency of the pores. However, more than 50 vol% of the FC-43 did not mix well with PDMS, leaving the phases separated from each other, like oil and water as aforementioned above. Based on these results, subsequent FEA and experiments used a dielectric layer made of 40 vol% FC-43.

PDMS films with pattern distances of 200 μm, 400 μm, and 600 μm were modeled based on Young's modulus measured from the tensile test. The patterns were considered to have the same Young's modulus as the film because the porous structures were also defined on the patterns (Supplementary Material Fig. S3). Tetrahedron mesh and solid element were used for both the film and pusher (Fig. 4(a)). The number of mesh with a pattern distance of 200 μm, 400 μm, and 600 μm were 247,086, 696,169, and 949,247, respectively. Each pattern had a bottom diameter of 100 μm, a top diameter of 30 μm, and a height of 100 μm. The pusher was modeled as a rigid body, and it moved downward as much as 200 μm (Fig. 4(b)). The bottom of the film was fixed, and the reaction force was calculated from the fixed part. The patterns were assumed to have exactly the same height, the bottom diameter, and the top diameter. They also were assumed to have the same porosity, resulting in the same Young's modulus.

To verify the validity of the analysis and patterns' behavior, a simple experiment with the same conditions was conducted; it showed nearly identical behavior under the same applied deformation (Fig. 5(a)). The cone-shape pattern easily buckles and deforms significantly even at low pressure, thus greatly improving the sensitivity of the sensor. Moreover, the reaction force also confirmed that the analysis showed almost the

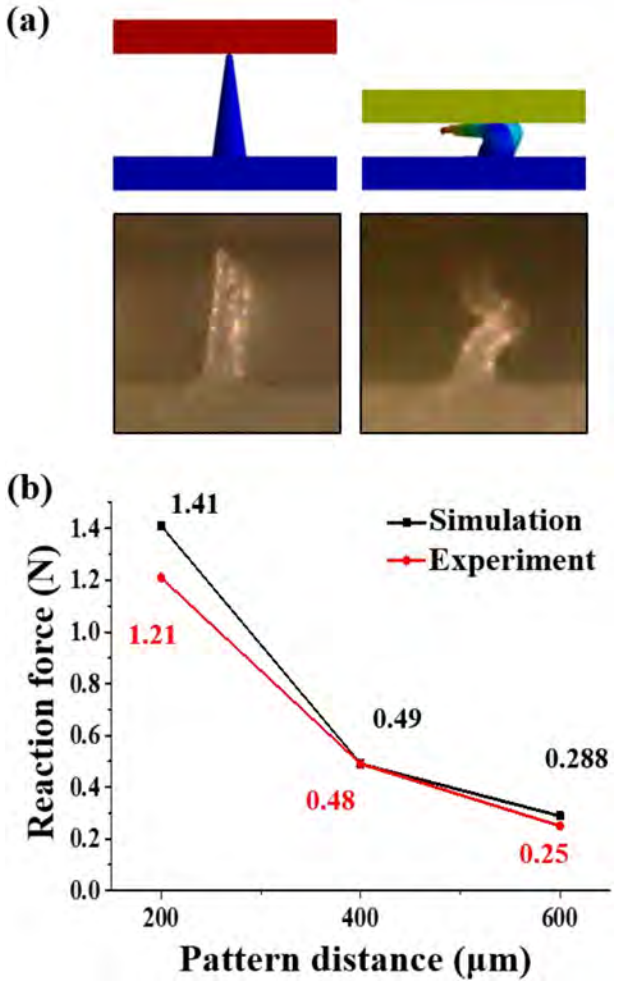

Fig. 5. (a) Comparison of pattern behavior of the FEA and experiment under compressive deformation. (b) Reaction forces measured from the FEA and experiment.

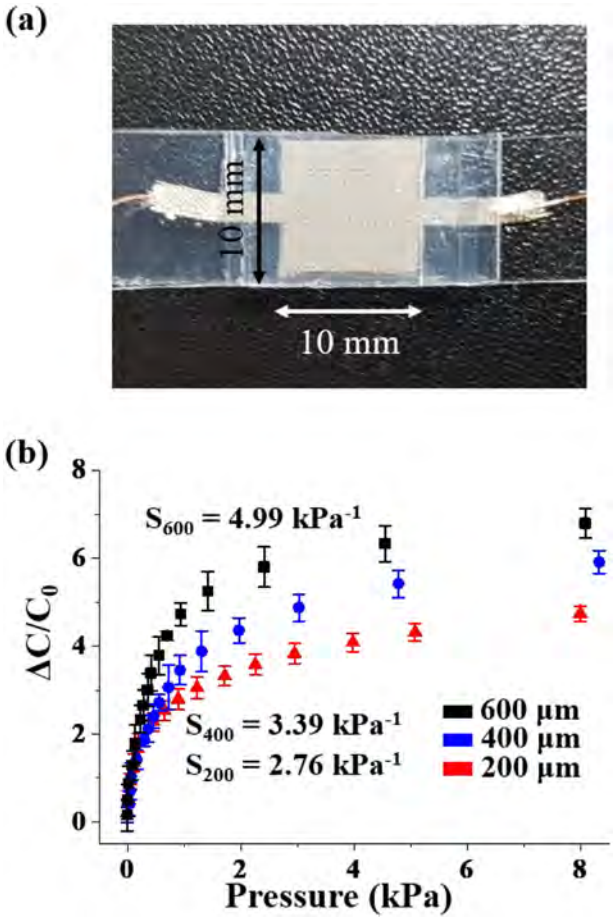

Fig. 6. (a) Image of the pressure sensor with proposed PDMS dielectric layer. (b) Capacitance change ratio of the pressure sensors with respect to the applied external pressure. The legend shows the pattern distance, and error bars indicate the standard deviations of the three samples.

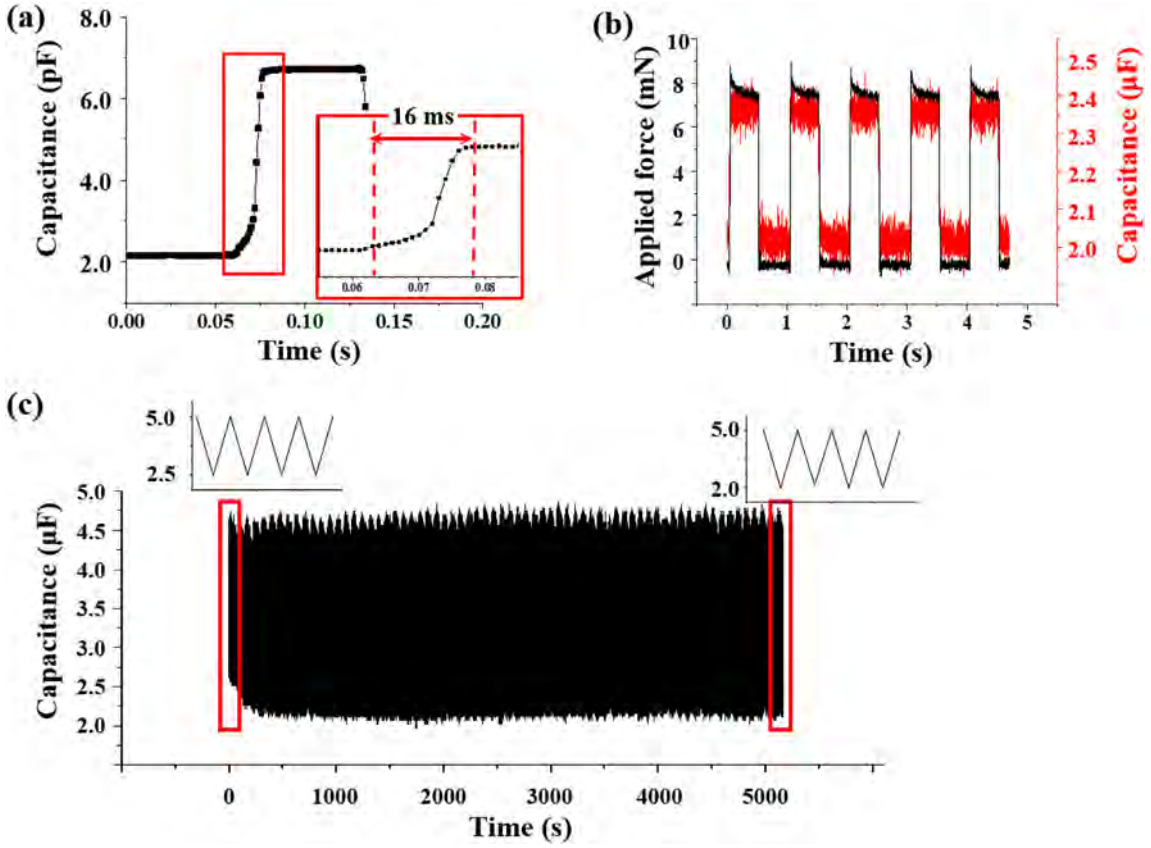

Fig. 7. (a) Response time of the sensor. (b) Mechanical response of the sensor under external periodic stimuli. (c) Durability test by cyclic loading pressure of 0.8 kPa.

same values, which means that the FEA was valid (Fig. 5(b)). The reaction forces obtained from experiments and FEA have almost the same value, and the error was within about 15%. The error may occur due to the assumption of the FEM models. In the case of 200 μm, the error was the largest, possibly due to a defect in the pattern tearing during peeling off of the fabrication process. It may also due to several assumptions used when conducting the analysis. However, the trends of experiments and FEA agree well with each other; as the distance of the pattern increased, the reaction force exponentially decreased (also see Supplementary Material Video S1, Fig. S4, and Fig. S5). A smaller reaction force indicates that more deformation would occur under the same applied force. That is, the deformability of the film could be improved by increasing the pattern distance. A small reaction force with the same variation of d indicates the sensor has high sensitivity. The sensitivity of a capacitive pressure sensor is calculated by dividing the capacitance change ratio by the applied pressure, and the capacitance is inversely proportional to the distance between the two electrodes.

3.3. Performances of pressure sensors

We manufactured capacitive pressure sensors to measure the capacitance change ratio under pressure with respect to the pattern distance (Fig. 6(a)). The PDMS layer was prepared by mixing 40 vol % of FC-43 due to the highest deformability (please refer to the Supplementary Material Fig. S6 and S7). The sensors were pressed at a speed of 10 μm/s using a motorized *Z*-stage. The capacitance change ratio and pressure were calculated from the measured capacitance and reaction force, respectively. The effective sensing area of the sensors was 10 mm by 10 mm. The pressure was applied up to 8 kPa; the standard deviations of the three samples are shown in the graph. The sensitivity of the sensor was calculated up to 0.2 kPa. As we expected, the sensitivity of the sensor increased significantly as the pattern distance increased. In particular, the sensitivity for 600 μm was 1.8 times greater than that for 200 μm (Fig. 6(b)). Through the proposed method in this study, highly sensitive capacitive pressure sensors could be fabricated in several minutes (please refer to the Supplementary Material Table S1). Meanwhile, all three curves were divided into two regions like a bi-linear function.

This phenomenon can be explained by three factors. The main factor is the buckling of the patterns. Since the patterns had high aspect ratios, they were easily buckled by the force exerted on the pattern. The pattern did not play any role in terms of deformability after the patterns lied down on the surface of the layer; thus, the sensitivity of the sensor rapidly decreased in high-pressure regions. The shape of the pores inside the layer under pressure also changed. When the external pressure was applied, the pore began to close. Since Young's modulus of the pores may be negligible, undeformed PDMS film with pores is much softer than a solid PDMS film. Thus, it is much easier to deform the PDMS film in a lower-pressure region, which leads to a greater change in capacitance. However, a pore's deformation becomes severe as the pressure increases, and it becomes flatter. At this moment, the deformed porous PDMS film would have the almost same Young's modulus as a solid PDMS film. As a result, the change in capacitance value is also reduced in high-pressure regions. Similarly, as the sensor is pressed, the volume fraction of the air (which has a lower dielectric constant than PDMS) decreases, and thus the effective dielectric constant of the layer increases. When the applied pressure reaches a certain value, the dielectric constant no longer changes. The capacitance change ratio should be much lower in this circumstance.

We conducted additional experiments to investigate the sensor's response to external pressure. The response time of the sensor is one of the critical factors in expanding the range of potential applications. The response time was defined as the time interval of 10% through 90% of the steady-state value [22,26]. As shown in Fig. 7(a), when the

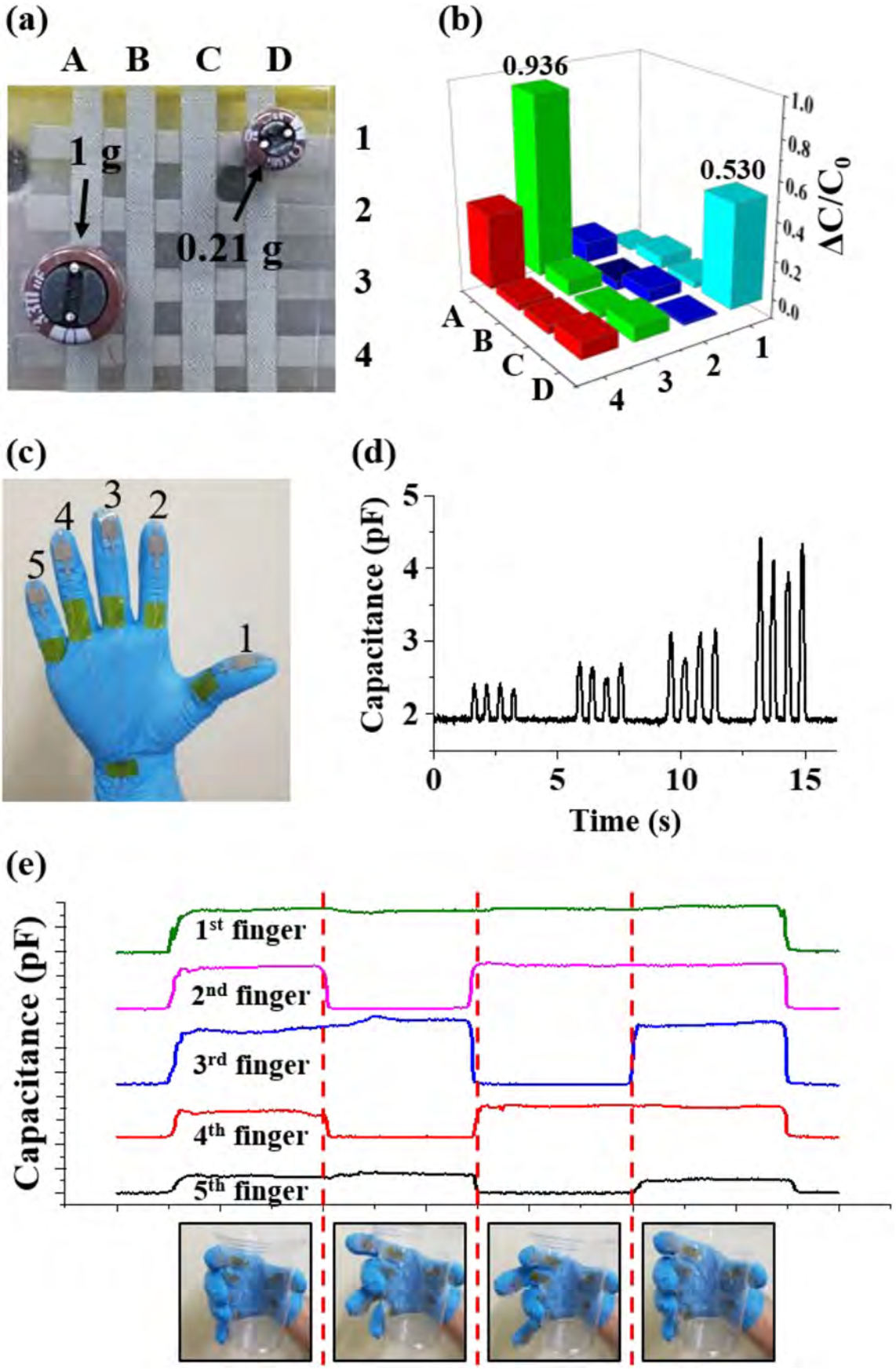

Fig. 8. (a) and (b) 0.21-g and 1-g weights were placed on the sensor array, and the resulting capacitance change ratio is shown. (c) Five sensors on each finger were used to mimic human skin. (d) Output signals from a finger-tapping test using the second finger. (e) Output signals of the five sensors under static and dynamic external stimuli.

sensor was pressurized with a pressing speed of 10 mm/s, fast response time of 16 ms was observed, which is highly advantageous for detecting high-frequency human motions. A sensor with a fast response time and high sensitivity can be used in a wide range of applications, including surgical robots and heart rate monitoring systems. In addition, we conducted an experiment to measure the hysteresis of the sensor using the pattern distance of 600 μm and the ratio of the sacrificial solvent of 40 vol%. As can be seen from Supplementary Material Fig. S8, the hysteresis of the sensor is sufficiently small. This small hysteresis may be attributed to the viscoelastic behavior of the PDMS film. When the periodic force is applied, the output signals generally follow the same shapes as that of the driving signals, showing a minimal delay (Fig. 7(b)). It was assumed that the reaction force would slightly decrease with time due to the viscoelastic properties of PDMS [35–37]. The robustness of the sensor is also an important factor. Our sensor showed a stable output signal for up to 5000 cycles with the frequency of 1 Hz for 5000 s at an applied pressure of 0.8 kPa, as shown in Fig. 7(c).

3.4. Applications

Several confirmatory experiments were carried out for future applications. Fig. 8(a) shows a 4 × 4 sensor array with 3 mm × 3 mm pixels. Accurately detecting the pressure distribution is a critical factor for measuring fine movements as an artificial skin. We placed a 0.21 g object on the D1 position of the array and a 1 g object between A3 and A4, slightly offset to A3. The pressures exerted by the objects were well identified as shown in Fig. 8(b)). A3 showed a larger capacitance change ratio than A4 because the object was closer to A3. Compared with the applied pressure, the capacitance change ratio was slightly smaller because the pressures applied by the objects were distributed to areas beyond the electrodes. Furthermore, our sensor can be easily extended to a sensor array by fabricating a film and cutting it to a size that overs all the pixels.

We also demonstrated the measurements of the static and dynamic pressures to apply it as an artificial skin. First, we attached five sensors onto fingers, as shown in Fig. 8(c), with an effective sensing area of $10 \times 10\ mm^2$, then consecutively tapped a table surface with the second finger. Several sets of tapping were conducted with increasing pressure. The table was tapped four times with similar pressure in each set (Fig. 8 (d) and also see Supplementary Material Fig. S9). The sensor detected each tapping well. The results of these experiments indicated that our sensor can measure the applied dynamic and static pressures quickly. Besides, when no pressure was applied, the capacitance value rapidly decreased to its base value and maintained stable output signals, which shows the excellent stability of our sensor.

Finally, we lifted a plastic cup weighing about 10 g with five fingers (Fig. 8(e) and also watch Supplementary Material Video S2). Then, the fingers holding the cup were changed to measure the signals of the sensors in response to the dynamic and static pressures. To evaluated the sensor's performance in response to static and dynamic pressure, we picked up a plastic cup weighing 10 g with five fingers. Each sensor was attached to finger holding the cup by following steps: (1) keep the five fingers holding the cup for 3 s; (2) lift the second and fourth fingers from the cup; (3) hold the stat of (2) for 3 s; (4) pick up the cup with the second and fourth fingers and simultaneously lift the third and fifth fingers out of the cup; (5) hold the state of (4) for 3 s; (6) pick up the cup with all five fingers; (7) hold the state of (6) for 3 s; and (8) release the cup. As shown in the graph, the pressure exerted on the sensors attached to each finger was well represented by the change in capacitance value. Each sensor responded well to static motion or dynamic motion; it was confirmed that the increase, maintenance, and decrease of the capacitance value were well detected. These demonstrations indicate that the proposed pressure sensor could be applied to artificial skin, medical instruments, the pressure distribution of an object (e.g., baseball bats, balls, runner's shoes, and chairs), and pressure monitoring systems.

4. Conclusion

In summary, we proposed a flexible and highly sensitive capacitive pressure sensor using a porous structured PDMS dielectric layer with cone-shaped patterns fabricated by simple microwave irradiation. The sacrificial solvent ratio directly affected the pore size and porosity, which in turn strongly influenced the deformability of the dielectric layer. Moreover, as the pattern distance increased, the reaction force under the same applied deformation decreased, resulting in higher sensitivity of the pressure sensors. A sensitivity as high as $4.99\ kPa^{-1}$ was obtained at a solvent ratio of 40 vol% and a pattern distance of 600 μm due to the combined effect of enhanced deformability and a varying effective dielectric constant of the dielectric layer. The sensors showed a fast response time of 16 ms and stable output signals during the cyclic test of 5000 cycles. The proposed sensor was also confirmed to be suitable as an artificial skin by measuring the static and dynamic pressure of the sensor array and finger-attached sensors. The proposed pressure sensor with porous structures and cone-shaped patterns can be easily expanded to large-area sensor arrays or skin-attachable sensors, allowing it to be used in soft, flexible, and stretchable electronics.

Supplementary data to this article can be found online at https://doi.org/10.1016/j.matdes.2020.109203.

Declaration of Competing Interest

There are no conflicts to declare.

Acknowledgements

This work was supported by the National Research Foundation of Korea (NRF) grant, funded by the Korea Government (MSIP) (No. 2019R1A2C1005023). This work was also supported by the research fund of Hanyang University (HY-2020-0389).

References

[1] M.D. Wales, P. Clark, K. Thompson, Z. Wilson, J. Wilson, C. Adams, Multicore fiber temperature sensor with fast response times, OSA Continuum 1 (2) (2018) 764–771.
[2] M.A. Hernández-Rodrguez, A.D. Lozano-Gorrín, I.R. Martín, U.R. Rodríguez-Mendoza, V. Lavín, Comparison of the sensitivity as optical temperature sensor of nano-perovskite doped with Nd^{3+} ions in the first and second biological windows, Sensors Actuators B Chem. 255 (2018) 970–976.
[3] J. Dai, H. Zhao, X. Lin, S. Liu, Y. Liu, X. Liu, T. Fei, T. Zhang, Ultrafast response polyelectrolyte humidity sensor for respiration monitoring, ACS Appl. Mater. Interfaces 11 (6) (2019) 6483–6490.
[4] Y. Pang, J. Jian, T. Tu, Z. Yang, J. Ling, Y. Li, X. Wang, Y. Qiao, H. Tian, Y. Yang, T.L. Ren, Wearable humidity sensor based on porous graphene network for respiration monitoring, Biosens. Bioelectron. 116 (2018) 123–129.
[5] Z. Yang, Y. Pang, X.L. Han, Y. Yang, J. Ling, M. Jian, Y. Zhang, Y. Yang, T.L. Ren, Graphene textile strain sensor with negative resistance variation for human motion detection, ACS Nano 12 (9) (2018) 9134–9141.
[6] X. Dong, H. Du, X. Sun, Z. Luo, J. Duan, A novel strain sensor with large measurement range based on all fiber mach-zehnder interferometer, Sensors (Basel) 18 (5) (2018) 1549–1550.
[7] R. Li, Y. Si, Z. Zhu, Y. Guo, Y. Zhang, N. Pan, G. Sun, T. Pan, Supercapacitive iontronic nanofabric sensing, Adv. Mater. 29 (36) (2017) 1700253.
[8] G.Y. Bae, J.T. Han, G. Lee, S. Lee, S.W. Kim, S. Park, J. Kwon, S. Jung, K. Cho, Pressure/temperature sensing bimodal electronic skin with stimulus discriminability and linear sensitivity, Adv. Mater. 30 (43) (2018) 1803388.
[9] W.A.D.M. Jayathilaka, K. Qi, Y. Qin, A. Chinnappan, W. Serrano-Garcia, C. Baskar, H. Wang, J. He, S. Cui, S.W. Thomas, S. Ramakrishna, Significance of nanomaterials in wearables: a review on wearable actuators and sensors, Adv. Mater. 31 (7) (2019) 1805921.
[10] J.S. Heo, J. Eom, Y.H. Kim, S.K. Park, Recent progress of textile-based wearable electronics: a comprehensive review of materials, devices, and applications, Small 14 (3) (2018) 1703034.
[11] T.T. Pham, H. Zhang, S. Yenuganti, S. Kaluvan, J.A. Kosinski, Design, modeling, and experiment of a piezoelectric pressure sensor based on a thickness-shear-mode crystal resonator, IEEE Trans. Ind. Electron. 64 (11) (2017) 8484–8491.
[12] H.J. Kim, Y.J. Kim, High performance flexible piezoelectric pressure sensor based on CNTs-doped 0-3 ceramic-epoxy nanocomposites, Mater. Des. 151 (2018) 133–140.

[13] Z. Chen, Z. Wang, X. Li, Y. Lin, N. Luo, M. Long, N. Zhao, J.B. Xu, Flexible piezoelectric-induced pressure sensors for static measurements based on nanowires/graphene heterostructures, ACS Nano 11 (5) (2017) 4507–4513.
[14] D.Y. Park, D.J. Joe, D.H. Kim, H. Park, J.H. Han, C.K. Jeong, H. Park, J.G. Park, B. Joung, K.J. Lee, Self-powered real-time arterial pulse monitoring using ultrathin epidermal piezoelectric sensors, Adv. Mater. 29 (37) (2017) 1702308.
[15] H. Kim, F. Torres, Y. Wu, D. Villagran, Y. Lin, T.-L. Tseng, Integrated 3D printing and corona poling process of PVDF piezoelectric films for pressure sensor application, Smart Mater. Struct. 26 (2017), 085027, .
[16] N. Nan, D.B. DeVallance, Development of poly(vinyl alcohol)/wood-derived biochar composites for use in pressure sensor applications, J. Mater. Sci. 52 (2017) 8247–8257.
[17] D. Lee, S. Cho, H. Ryu, Y. Pu, S.-S. Yoo, M. Lee, K.C. Hwang, Y.Y. Youngoo, K.-Y. Lee, A highly linear, AEC-Q100 compliant signal conditioning IC for automotive piezo-resistive pressure sensors, IEEE Trans. Ind. Electron. 65 (9) (2018) 7363–7979.
[18] H. Jeong, Y. Noh, S.H. Ko, D. Lee, Flexible resistive pressure sensor with silver nanowire networks embedded in polymer using natural formation of air gap, Compos. Sci. Technol. 174 (2019) 50–57.
[19] S. Chen, Y. Song, F. Xu, Flexible and highly sensitive resistive pressure sensor based on carbonized crepe paper with corrugated structure, ACS Appl. Mater. Interfaces 10 (40) (2018) 34646–34654.
[20] J. Pan, S. Liu, Y. Yang, J. Lu, A highly sensitive resistive pressure sensor based on a carbon nanotube-liquid crystal-PDMS composite, Nanomaterials (Basel) 8 (6) (2018) 413.
[21] C. Jeong, J.S. Lee, B. Park, C.S. Hong, J.U. Kim, T.I. Kim, Controllable configuration of sensing band in a pressure sensor by lenticular pattern deformation on designated electrodes, Adv. Mater. 31 (36) (2019) 1902689.
[22] Y. Kim, S. Jang, B.J. Kang, J.H. Oh, Fabrication of highly sensitive capacitive pressure sensors with electrospun polymer nanofibers, Appl. Phys. Lett. 111 (2017), 073502, .
[23] J. Lee, H. Kwon, J. Seo, S. Shin, J.H. Koo, C. Pang, S. Son, J.H. Kim, Y.H. Jang, D.E. Kim, T. Lee, Conductive fiber-based ultrasensitive textile pressure sensor for wearable electronics, Adv. Mater. 27 (15) (2015) 2433.
[24] S.W. Park, P.S. Das, A. Chhetry, J.Y. Park, A flexible capacitive pressure sensor for wearable respiration monitoring system, IEEE Sensors J. 17 (20) (2017) 6558–6564.
[25] Z. He, W. Chen, B. Liang, C. Liu, L. Yang, D. Lu, Z. Mo, H. Zhu, Z. Tang, X. Gui, Capacitive pressure sensor with high sensitivity and fast response to dynamic interaction based on graphene and porous nylon networks, ACS Appl. Mater. Interfaces 10 (15) (2018) 12816–12823.
[26] Y. Kim, S. Jang, J.H. Oh, Fabrication of highly sensitive capacitive pressure sensors with porous PDMS dielectric layer via microwave treatment, Microelectron. Eng. 215 (2019) 111002.
[27] S. Baek, H. Jang, S.Y. Kim, H. Jeong, S. Han, Y. Jang, D.H. Kim, H.S. Lee, Flexible piezocapacitive sensors based on wrinkled microstructures: toward low-cost fabrication of pressure sensors over large areas, RSC Adv. 7 (2017) 39420–39426.
[28] M.-F. Lin, J. Xiong, J. Wang, K. Parida, P.S. Lee, Core-shell nanofiber mats for tactile pressure sensor and nanogenerator applications, Nano Energy 44 (2018) 248–255.
[29] A. Chhetry, H. Yoon, J.Y. Park, A flexible and highly sensitive capacitive pressure sensor based on conductive fibers with a microporous dielectric for wearable electronics, J. Mater. Chem. C 5 (2017) 10068–10076.
[30] J.I. Yoon, K.S. Choi, S.P. Chang, A novel means of fabricating microporous structures for the dielectric layers of capacitive pressure sensor, Microelectron. Eng. 179 (2017) 60–66.
[31] J. Wang, R. Suzuki, M. Shao, F. Gillot, S. Shiratori, Capacitive pressure sensor with wide-range, bendable, and high sensitivity based on the bionic Komochi Konbu structure and Cu/Ni nanofiber network, ACS Appl. Mater. Interfaces 11 (2019) 11928–11935.
[32] P. Wei, X. Guo, X. Qiu, D. Yu, Flexible capacitive pressure sensor with sensitivity and linear measuring range enhanced based on porous composite of carbon conductive paste and polydimethylsiloxane, Nanotechnology 30 (2019) 455501.
[33] S. Kang, J. Lee, S. Lee, S. Kim, J.-K. Kim, H. Algadi, S. Al-Sayari, D.-E. Kim, D.E. Kim, T. Lee, Highly sensitive pressure sensor based on bioinspired porous structure for real-time sensing, Adv. Electron. Mater. 2 (2016) 1600356.
[34] D. Kwon, T.-I. Lee, J. Shim, S. Ryu, M.S. Kim, S. Kim, T.-S. Kim, I. Park, Highly sensitive, flexible, and wearable pressure sensor based on a giant piezocapacitive effect of three-dimensional microporous elastomeric dielectric layer, ACS Appl. Mater. Interfaces 8 (2016) 16922–16931.
[35] A. Dalla Monta, F. Razan, J.-B. Le Cam, G. Chagnon, Using thickness-shear mode quartz resonator for characterizing the viscoelastic properties of PDMS during cross-linking, from the liquid to the solid state and at different temperatures, Sens. Actuator A Phys. 280 (2018) 107–113.
[36] A.S. Mijailovic, B. Qing, D. Fortunato, K.J. Van Vliet, Characterizing viscoelastic mechanical properties of highly compliant polymers and biological tissues using impact indentation, Acta Biomater. 71 (2018) 388–397.
[37] W.S. Lee, K.S. Yeo, A. Andriyana, Y.G. Shee, F.R. Mahamd Adikan, Effect of cyclic compression and curing agent concentration on the stabilization of mechanical properties of PDMS elastomer, Mater. Des. 96 (2016) 470–475.